

Development of a Millimeter-Wave Transducer for Quantum Networks

Kevin K. S. Multani^{1,3}, Hubert Stokowski^{2,3}, Emma Snively⁴, Rishi Patel^{2,3}, Wentao Jiang^{2,3}, Nathan Lee^{2,3}, Paul B. Welander⁴, Emilio A. Nanni⁴, Amir H. Safavi-Naeini^{2,3}

¹Stanford University, Department of Physics, Stanford, CA 94305, USA

²Stanford University, Department of Applied Physics, Stanford, CA 94305, USA

³Stanford University, Ginzton Laboratory, 348 Via Pueblo Mall, Stanford, CA 94305, USA

⁴SLAC National Accelerator Laboratory, 2575 Sand Hill Rd, Menlo Park, CA 94025, USA

Abstract — Proliferation of superconducting quantum technology is limited by the scalability of such systems. Networking physically separated quantum processors is seen as a potential solution to the scalability problem. We previously proposed a microwave-millimeter four-wave mixing transduction scheme, which potentially provides a way to link quantum systems through a channel at liquid helium temperatures (4 K). In this work, we present a design methodology and measurements of a superconducting device that supports two independent modes separated by 55 GHz.

I. INTRODUCTION

SUPERCONDUCTING QUANTUM processors remain to be networked like their classical counterparts. Networking these quantum systems would allow entanglement to be distributed between physically separated quantum processors. This serves as a solution to the scalability problem the technology currently faces. One approach towards networking is to directly connect two dilution refrigerators using microwave waveguides (~5 GHz) that are cooled down to millikelvin temperatures¹. Another way is to use microwave-millimeter-wave interconnects, which requires a transducer to convert signals from microwave to millimeter-wave frequencies. These interconnects can enable quantum links at liquid Helium temperatures (4 K) such that local, high-bandwidth quantum networks can be established². The device presented in this article is a step in realizing a microwave-millimeter wave transducer, building on previous work^{2,3,4}.

Driven by a kinetic inductance nonlinearity, we aim to use four-wave mixing to perform the transduction between one microwave photon (~5 GHz) and one mm-wave photon (~105 GHz), by using two pump photons with frequency: $\omega_p = (\omega_{mm} - \omega_{\mu m})/2$. Our previous work showed a device that supports the millimeter-wave mode³, here we present an example of a device that supports the millimeter-wave mode (~105 GHz) and the pump-mode (~50 GHz).

II. DESIGN

The two-mode resonator design builds on our previous work, where we consider a thin-film Niobium superconducting device with a single resonance³. To recap, we model the resonator as a dipole interacting with the impinging fields in a rectangular waveguide, so there are only two parameters of interest: the effective dipole length and the length of the resonator. These two parameters influence the external coupling and resonance frequency, respectively. When designing the next iteration of devices, we need to consider one additional factor – the overlap of the spatial current distribution between the modes. In the microwave-mm-wave transduction scheme², the conversion

rate is directly proportional to the spatial current overlap between the microwave mode, pump mode, and mm-wave mode. In particular,

$$g_0 \propto \phi_{mm} \phi_{\mu m} \phi_p^2 \propto \left(\int_{\Omega} J_{mm}^n dA \right) \left(\int_{\Omega} J_{\mu m}^m dA \right) \left(\int_{\Omega} J_p^n dA \right)^2,$$

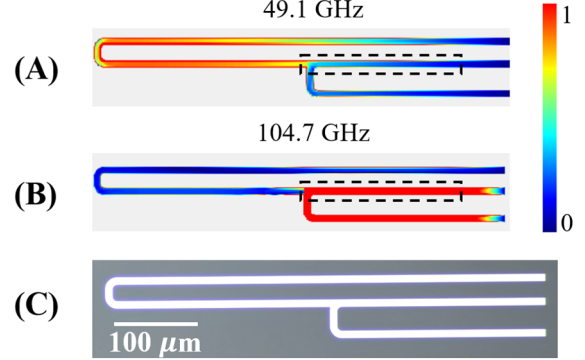


Fig. 1. (A, B) SONNET-simulated normalized current distributions and resonance frequencies of the measured device shown in (C). The boxed region in (A) and (B) indicate where the current distributions overlap. (A) Normalized current distribution for a mode with a resonance frequency of 49.1 GHz. (B) Normalized current distribution for a mode with a resonance frequency of 104.7 GHz. (C) Optical microscope image of the measured device. The bright areas are 200 nm thick Niobium film and the dark areas

where g_0 is the conversion rate and ϕ_i are the vacuum fluctuation amplitudes of the flux variables for each of the respective modes. The J_i^n 's represent the normal component of the spatial current density distribution of mode i and Ω is the geometry of the resonator. Engineering g_0 directly is important as it is directly related to conversion efficiency, specifically, it can approach unity when²:

$$\frac{g_0^2 n_p^2}{\kappa_{mm} \kappa_{\mu m}} = 1,$$

where the κ_i 's are the external coupling of the respective modes and n_p is the number of pump photons (proportional to pump power). Using the principles described, we designed and fabricated various geometries which supports the millimeter-wave mode (~105 GHz) and the pump mode (~50 GHz). We simulated these geometries in a full-wave electromagnetic solver (SONNET), to calculate the current density profiles. To select between geometries, one needs to maximize the current density overlap. An example of a geometry with high overlap is shown in Figure 1.

III. EXPERIMENT AND RESULTS

We fabricated several devices using photolithography, with an Argon ion-milling procedure to etch the pattern, followed by an Oxygen plasma clean. For the remainder of this article, we focus on the device shown in Figure 1(C). To measure this

device, we set up the measurement chain depicted in Figure 2. The goal was to measure the pump mode and millimeter-wave mode of the same device in one cooldown. We achieved this by mounting WR15 components inside of our closed-cycle Helium cryostat (Montana Instruments Nanoscale Workstation) and swapped between WR15 and WR10 components outside of the cryostat. As a result, the WR15 components inside of the cryostat were operated in an overmoded fashion. To properly terminate the measurement chain, we mounted a short-circuit cap provided in the calibration kit for the frequency extenders (Virginia Diodes Inc.).

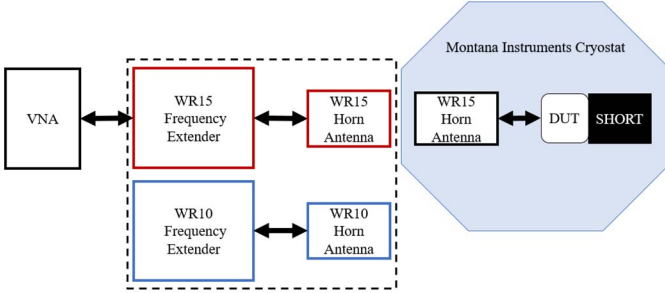


Fig. 2. Measurement chain for the experiment. The black arrows represent a transmission line component where the length is greater than the free-space wavelength of the signals. We measure the same device in two bands by switching between the WR15 components outside of the cryostat by WR10 components. Components inside of the cryostat experience temperatures as low as 4.1 K, and pressures as low as 10^{-6} hPa. The DUT is the device shown in Fig. 1(C). The SHORT component is a short-circuit termination provided in the WR15 extender calibration kit (Virginia Diodes Inc.).

Using this scheme, we measured reflection spectra of the pump mode and the millimeter-wave mode as a function of temperature. We normalize the data to the highest temperature (12 K) to remove most of the background and weak resonances present in the measurement chain. Figure 3 summarizes these measurements. We observe the resonances redshift and eventually disappear as the temperature rises, which is a signature of superconducting resonators. From our measurements we find that the transition temperature is somewhere between 8-9 K, as expected from thin-film Niobium⁴.

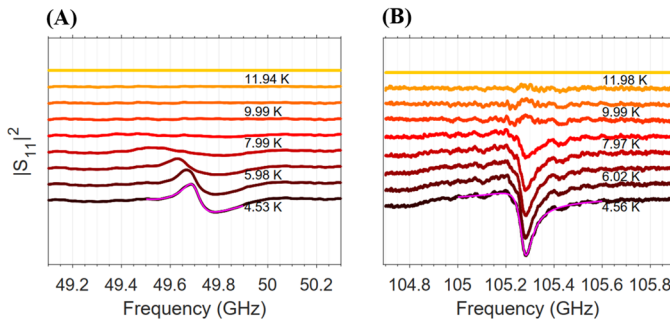


Fig. 3. Reflection spectra of the pump mode and the millimeter-wave mode as a function of temperature of the device presented in Fig. 1(C). The data have been normalized by the highest temperature spectra. The lowest temperature data have been fit, indicated by the magenta curve. (A) The resonance frequency given by the fit is 49.7 GHz. (B) The resonance frequency given by the fit is 105.3 GHz.

The lowest temperature measurements were fit using the complex valued S-parameter data⁵ to account for asymmetric line-shapes accurately. We find the pump mode to have a resonance frequency of 49.7 GHz, a total quality factor of 5.6×10^2 , and an external quality factor of 1.9×10^4 . For the millimeter-wave mode we find a resonance frequency of 105.3 GHz, a total quality factor of 1.7×10^3 , and an external quality factor of 1.7×10^4 .

IV. DISCUSSION

Figure 3 shows that the pump-mode disappears at a lower temperature than the millimeter-wave mode. This observation is commensurate with the pump-mode having a lower quality factor. Furthermore, we find that the resonance frequencies differ from simulated values by 1.22% (600 MHz) for the pump mode and 0.573% (600 MHz) for the millimeter-wave mode. These small discrepancies fall well within disorder introduced in the fabrication process.

V. CONCLUSION

In short, we present progress in the design methodology of superconducting devices that utilize the kinetic inductance nonlinearity for transduction of microwave quanta to millimeter-wave quanta (and vice-versa). As a first step to test this new design process, we present an example of a doubly resonant device with high current density overlap. In the near-term, two-tone measurements will be conducted to characterize the strength of the non-linear interaction. In the future, we will integrate the full microwave-millimeter-wave transducer with transmon qubits to establish high-bandwidth local quantum networks.

ACKNOWLEDGEMENTS

E. A. N. acknowledges support by the Department of Energy contract DEAC0276SF00515 and by NSF grant PHY-1734015. A. H. S-N. acknowledges support from the David and Lucille Packard Fellowship. Work was performed in part in the nano@Stanford labs, which are supported by the National Science Foundation as part of the National Nanotechnology Coordinated Infrastructure under award ECCS-1542152. Part of this work was performed at the Stanford Nano Shared Facilities (SNSF), supported by the National Science Foundation under award ECCS-1542152.

REFERENCES

- [1] S. Storz, et al., “Experimental Study of an Elementary Cryogenic Microwave Quantum Network,” presented at the *APS March Meeting 2020*, Denver, CO, USA, Mar. 2-6, 2020.
- [2] M. Pechal, and A. H. Safavi-Naeini, “Millimeter-wave interconnects for microwave-frequency quantum machines,” *Phys. Rev. Applied* **96**, pp. 042305-1-13, Oct. 2017, doi: [10.1103/PhysRevA.96.042305](https://doi.org/10.1103/PhysRevA.96.042305)
- [3] H. Stokowski, et al., “Towards Millimeter-Wave Based Quantum Networks,” in *IRMMW-THz 2019*, Paris, France, 2019, pp. 1-2, doi: [10.1109/IRMMW-THz.2019.8874171](https://doi.org/10.1109/IRMMW-THz.2019.8874171)
- [4] A. Anfermov, et al., “Millimeter-Wave Four-Wave Mixing via Kinetic Inductance for Quantum Devices,” *Phys. Rev. Applied* **13**, 024056, Feb. 21, 2020, doi: doi.org/10.1103/PhysRevApplied.13.024056
- [5] J. R. Rairden, C. A. Neugebauer, “Critical temperature of niobium and tantalum films,” *Proc. IEEE*, vol. 52, pp. 1234-1238, Oct. 1964
- [6] M. S. Khalil, et al., “An analysis method for asymmetric resonator transmission applied to superconducting devices,” *Journal of Applied Physics* **111**, 054510 (2012), doi: doi.org/10.1063/1.3692073